Physica C 501 (2014) 24–31

Contents lists available at ScienceDirect

Physica C

journal homepage: www.elsevier.com/locate/physc

Fluctuation conductivity and pseudogap in $HoBa_2Cu_3O_{7-\delta}$ single crystals under pressure with transport current flowing under an angle 45° to the twin boundaries

A.L. Solovjov [a,c], M.A. Tkachenko [a,c], R.V. Vovk [b], A. Chroneos [d,*]

[a] B.I. Verkin Institute for Low Temperature Physics and Engineering of National Academy of Science of Ukraine, 47 Lenin ave., 61103 Kharkov, Ukraine
[b] V.N. Karazin Kharkov National University, 4 Svobody sq., 61077 Kharkov, Ukraine
[c] International Laboratory of High Magnetic Fields and Low Temperatures, 95 Gajowicka Str., 53-421 Wroclaw, Poland
[d] Department of Materials, Imperial College, London SW7 2AZ, United Kingdom

ARTICLE INFO

Article history:
Received 18 January 2014
Accepted 3 March 2014
Available online 1 April 2014

Keywords:
Fluctuation conductivity
Pseudogap
Single crystals
Pressure
Twin boundaries

ABSTRACT

The influence of hydrostatic pressure up to 0.48 GPa on the fluctuation conductivity $\sigma'(T)$ and pseudogap (PG) $\Delta^*(T)$ of slightly doped $HoBa_2Cu_3O_{7-\delta}$ single crystals with $T_c \approx 62$ K and $\delta \approx 0.35$ is studied with current passing under an angle 45° to the twin boundaries. It is shown that near T_c the conductivity $\sigma'(T)$ is well described by the Aslamasov–Larkin and Hikami–Larkin fluctuation theories demonstrating 3D–2D crossover with the increase of temperature. $\Delta^*(T)$ displays two representative maxima at $T_{max1} \approx 219$ K and $T_{max2} \approx 241$ K likely caused by the phase stratification of the single crystal. Pressure leads to disappearance of these maxima and linear $\Delta^*(T)$ with a positive gradient at high temperatures. Essentially, with the removal of pressure the maxima are restored. The comparison of our results with those obtained for $YBa_2Cu_3O_{7-\delta}$ sheds more light on the role of magnetic subsystem in the high-T_c superconductors.

1. Introduction

Superconductivity in high-temperature superconductors (HTS's) can be understood by studying their properties in the normal state, which are well known to be very peculiar [1–11]. The most intriguing property is a pseudogap (PG) observed mostly in oxygen deficient cuprates below any representative temperature $T^* \gg T_c$ (transition temperature) [5–9]. Many proposals have been presented to explain this phenomenon [7–9], including various forms of electron pairing [12–14], antiferromagnetic fluctuations [3,15] and spin-charge separation scenarios [16,17]. Nevertheless, in spite of intensive studies, the origin of the pseudogap is controversial. Notably, most models explain both the linear $\rho(T)$, observed in HTS's at $T > T^*$ [18], and anomalous Hall effect [9,19] but fail to account for all effects observed in experiment.

In a previous study [20] the fluctuation conductivity (FLC) and PG in $HoBa_2Cu_3O_{7-\delta}$ single crystals were investigated with a transport current passing in parallel to the twin boundaries. The results were treated within a model based on a conception of the local pairs (LP) which are believed to be in existence in HTS's below T^* [9,12–14,21]. Importantly, the LP model is able to explain the majority of peculiar effects being inherent in HTS's behavior [9,21]. Two peaks of $\Delta^*(T)$ were found which disappeared under pressure [20]. Simultaneously the $\Delta^*(T)$ dependence became linear with negative-gradient slope being typical for magnetic superconductors [22–24]. That is why we have proposed this negative-slope linearity to be due to internal magnetism of $HoBa_2Cu_3O_{7-\delta}$ cuprate caused by the inherent magnetism of holmium atoms with $\mu_{eff} = 10.6\mu_B$ (and $9.7\mu_B$ for $HoBa_2Cu_3O_{7-\delta}$) [25].

Substitution of Y in single crystals of $ReBa_2Cu_3O_{7-\delta}$ (Re = Y, Ho, Dy, etc.) with Ho of a fairly large magnetic moment suggests a change in behavior of the system due to paramagnetic properties of $HoBa_2Cu_3O_{7-\delta}$ in its normal state [25]. Samples exhibiting oxygen nonstoichiometry are of special interest. In this state the redistribution of labile oxygen and structural relaxation take place simultaneously, thus significantly affecting electron transport parameters of the system [26,27]. In this case rare alkaline earth metal ion can serve as a sensor, sensitive to local symmetry of its surroundings and charge density distribution, which can be affected by outside factors such as temperature [26] or high pressure [27].

Pressure has played an important role in the study of HTS's since the observation by Chu et al. [28] of a large pressure dependence of T_c in the La–Ba–Cu-0 system. In contrast to conventional superconductors dT_c/dP for the high-T_c superconductors appears to

* Corresponding author.
E-mail address: alexander.chroneos@imperial.ac.uk (A. Chroneos).

http://dx.doi.org/10.1016/j.physc.2014.03.004
0921-4534/

be in most cases positive whereas $d\ln\rho_{ab}/dP$ is negative and relatively large [29–31]. Applied pressure produces a reduction in lattice volume which promotes ordering and this appears to lead to positive dT_c/dP observed in experiment. The interpretation of the pressure effect on ρ is rather uncertain, since the nature of the transport properties for HTS's is not clear yet. The dominant contribution to the conductivity is known to come from the CuO_2 planes which are interconnected by a relatively weak transfer interaction. Most likely pressure leads to the increase in the charge concentration on the CuO_2 plane. The theoretical approach to the hydrostatic-pressure effects on the *a*-axis resistance of HTS's is discussed in Ref. [29]. There are also several papers in which the influence of pressure on the fluctuation conductivity was studied in a number of HTS's compounds [30–32]. But with the exception of our trials [20] no such studies are known to be performed in $HoBa_2Cu_3O_{7-\delta}$. Moreover, as far as we know no detailed study of pressure influence on pseudogap in high-T_c oxides has been carried out up to now.

In the present work we performed in-plane resistivity measurements under hydrostatic pressures up to $P = 0.48$ GPa on a slightly doped $HoBa_2Cu_3O_{7-\delta}$ (HoBCO) single crystal with $T_c = 61.3$ K at $P = 0$. Measurements were carried out with the flow of transport current under an angle 45° to the twin boundaries to clarify how the experiment geometry will affect the transport properties. We studied the fluctuations' contribution to the conductivity and focused on the temperature dependence of an excess conductivity $\sigma'(T)$. From the analysis of the excess conductivity the magnitude and temperature dependence of a pseudogap $(\Delta^*(T))$ with and without pressure were finally derived. The analysis was performed within our LP model [9,21] as discussed in details in the text. Comparison of our results with those obtained for $YBa_2Cu_3O_{7-\delta}$ (YBCO) [21,31], $Bi_2Sr_2CaCu_2O_{8+y}$ (BISCCO-2212) [30] and $HgBa_2Ca_2Cu_3O_8$ (Hg-2223) [32] may provide the substantial insight into the role of magnetic subsystem in the high-T_c cuprates.

2. Experiment

$HoBa_2Cu_3O_{7-\delta}$ single crystals were grown with the self-flux method in a gold crucible, as described elsewhere [26,33,34]. Our crystals are strongly twinned as a result of the samples annealing in an oxygen flow at a temperature of (370–410) °C for three to five days [35]. The annealing is used to obtain samples of appropriate oxygen content [26,27,35]. This procedure leads to the formation of the twin boundaries (**TB**) aligned through all the crystal (Fig. 1 in Ref. [33]), which effectively minimize the elastic energy of the crystal lattice in the tetragonal–orthogonal transition [27].

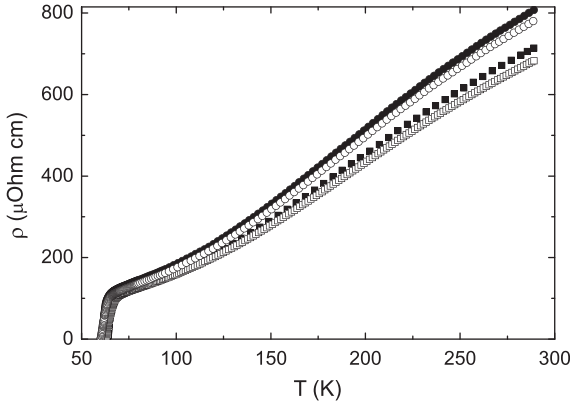

Fig. 1. In-plane resistivity of our HoBCO crystal as a function of *T*: dots – sample H21, $P = 0$; squares – H22, $P = 0.48$ GPa; open squares – H23, $P = 0.48$ GPa after 5 days under pressure; open circles – H24, $P = 0$ after removing pressure.

Rectangular crystals of about $1.7 \times 1.2 \times 0.2$ mm (sample S1) [20] and $1.9 \times 1.5 \times 0.3$ mm (sample S2) were selected from the same batch to perform the resistivity measurements. The smallest parameter of the crystal corresponds to the *c*-axis. The experimental geometry was selected so that the transport current vector in the *ab*-plane was either parallel, (**I**‖**TB**), (sample S1), or under an angle 45° (sample S2) to the **TB**. A fully computerized setup utilizing the four-point probe technique with stabilized measuring current of up to 10 mA was used to measure the *ab*-plane resistivity, $\rho_{ab}(T)$ [27]. Silver epoxy contacts were glued to the extremities of the crystal in order to produce a uniform current distribution in the central region where voltage probes in the form of parallel stripes were placed. Contact resistances below 1 Ω were obtained. The viewgraph of the sample morphology and the arrangement of contacts are discussed in details in Ref. [33]. Temperatures were measured with a Pt sensor having an accuracy about 1 mK. The hydrostatic pressure was generated inside a Teflon cup housed in a copper–beryllium piston-cylinder cell, as described in Ref. [36]. A manganin gauge made of a 25 Ω wire was used to determine the applied pressures. Transformer oil was used as the transmitting medium and pressures were changed at room temperature in the order of increasing magnitude. For each applied pressure, experimental runs were carried at rates of about 0.1 K/min near T_c and 0.5 K/min at $T \gg T_c$.

In order to determine the effect of oxygen redistribution, measurements were taken 2–7 days after applying–removing pressure, depending on completion of relaxation processes. Temperature dependencies of resistivity $\rho(T) = \rho_{ab}(T)$ for $HoBa_2Cu_3O_{7-\delta}$ single crystals with $T_c = 61.3$ K and $\delta \approx 0.35$ (sample S2) measured under various pressures and temperatures are shown in Fig. 1. All curves have an expected S-shape with positive thermally activated bending [33], characteristic for slightly doped cuprates [18,19]. However, above $T^* \sim 260$ K $\rho(T)$ varies linearly with T at rates $d\rho/dT = 3.1$ and $2.58\ \mu\Omega\,\mathrm{cm\,K^{-1}}$ for the pressures $P = 0$ and 0.48 GPa, respectively. (Note that 1 GPa = 10 kbar). The relative diminution of $\rho(T)$ as a function of pressure is practically temperature independent above 260 K and amounts to $d\ln\rho/dP = -4(\pm0.5)\%\ \mathrm{GPa^{-1}}$. This value is in agreement with results obtained for different cuprates [29–34]. Actually we have four curves (or fore samples) for the pressure $P = 0$ (Fig. 1, curve H21), 0.48 (curve H22), 0.48 applied for five days (curve H23) and again 0 GPa measured immediately after removing the pressure (curve H24). Fig. 2(a and b) shows the resistivity curves near T_c for $P = 0$ (a) and $P = 0.48$ GPa (b), respectively, in which all representative temperatures are designated. Besides, from Fig. 2 we deduce that T_c increases with pressure at a rate $dT_c/dP \approx +4\ \mathrm{K\,GPa^{-1}}$, which is noticeably larger than that obtained for optimally doped (OD) $YBa_2Cu_3O_{7-\delta}$ single crystals $(dT_c/dP \approx +1.3\ \mathrm{K\,GPa^{-1}})$ [31]. The result is in agreement with above idea as for enhancement of the charge carrier density (n_f) in CuO_2 planes under pressure. It appears that oxygen vacancies in slightly doped cuprates make the n_f rearrangement more easy to achieve.

Nevertheless, in spite of a number of studies on the relaxation processes in the 1–2–3 system under high pressure, many aspects, such as the charge transfer and the nature of the redistribution of the vacancy subsystem, still remain uncertain [31,33,34]. Thus, the electrical resistivity decreases not only as a consequence of the high pressure but also in the isobar process of retaining the sample at room temperature following the application of high pressure [33]. For example, in Fig. 1 curves H22 and H23 show the $\rho_{ab}(T)$ measured directly after the application of pressure ($P = 0.48$ GPa), as well as after the isobar process of retaining the sample at room temperature for five days under the pressure, respectively. This exposure leads to an additional decrease in electrical resistance of (4–5)%. Similar behavior of $\rho_{ab}(T)$ renewal was also observed in the process of the high pressure removal. Thus, in Fig. 1 curves

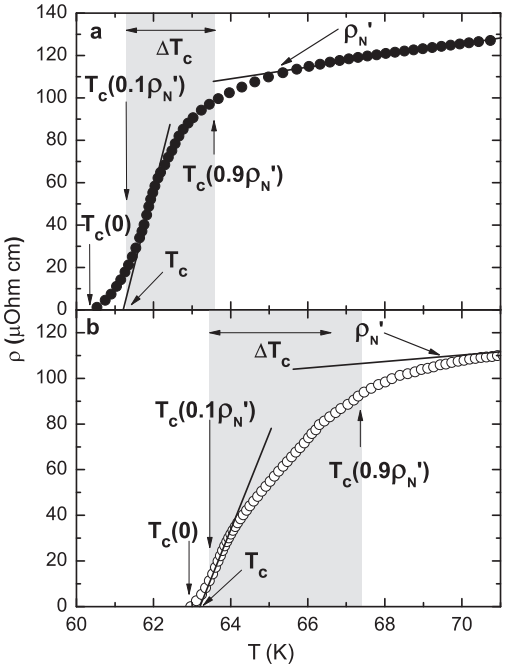

Fig. 2. Resistive transition of HoBCO single crystal at $P = 0$ (a) and $P = 0.48$ GPa (b).

H21 and H24 correspond to the ρ_{ab} vs T dependencies measured before the pressure application and immediately after its removal. Comparison of these curves indicates that the results depend on the duration of time the sample is at room temperature without pressure. Immediately after pressure removal, the value of electrical resistance of the sample at room temperature was approximately 4% less than the value measured prior to the application of pressure but gradually relaxed for three days to its equilibrium value. Thereafter, the ρ_{ab} (300 K) value saturates and finally the $\rho_{ab}(T)$ actually coincides with the original curve obtained before the application of pressure. This confirms the reversibility of the process. The sample S1 with **I**||**TB** behaves in a good many ways like those of sample S2. More detailed analysis of the resistivity curves for both samples is described elsewhere [33].

3. Results and discussion

3.1. Fluctuation conductivity

Measurements were performed with current flowing under an angle 45° to the twin boundaries when intensity of current carrier scattering should be enhanced as compared with the experimental geometry when current **I** is parallel to **TB** [20,27,33]. As clearly seen from Fig. 1 below the PG temperature $T^* = (265 \pm 0.2)$ K $\gg T_c$ resistivity of $HoBa_2Cu_3O_{7-\delta}$, $\rho(T)$, deviates down from linearity resulting in appearance of the excess conductivity

$$\sigma'(T) = \sigma(T) - \sigma_N(T) = [1/\rho(T)] - [1/\rho_N(T)], \quad (1)$$

where $\rho_N(T) = aT + \rho_0$ is the normal state resistivity extrapolated to low T region [3,37]. This procedure of the normal state resistivity determination is widely used in literature (see [37–41] and references therein) and has been justified theoretically by the Nearly Antiferromagnetic Fermi Liquid (NAFL) model [3]. The T^* temperature is taken at the point where the experimental resistance curve starts to downturn from the high-temperature linear behavior.

To determine T^* more precise $[\rho(T) - \rho_0]/aT$ criterium [19,41], where ρ_0 is the intercept with y-axis, was also used. Both approaches give practically the same T^*'s. The superconducting transition temperature T_c (Fig. 2) is determined by extrapolation of the linear part of the resistive transition to $\rho(T_c) = 0$ [40]. Here we focus on the analysis of fluctuation conductivity (FLC) and pseudogap (PG) derived from measured excess conductivity within our LP model. We will mainly perform the analysis for the sample H23 (sample S2 with $P = 0.48$ GPa applied for five days) and compare results with those obtained for the sample H21 (sample S2 with $P = 0$) as well as with results obtained for the sample S1 [20]. The determined from the analysis samples parameters are listed in the Tables 1 and 2.

To begin the analysis the mean field critical temperature T_c^{mf} has to be calculated. Here $T_c^{mf} > T_c$ is the critical temperature in the mean-field approximation, which separates the FLC region from the region of critical fluctuations or fluctuations of the order parameter Δ directly near T_c (where $\Delta < kT$), neglected in the Ginzburg–Landau (GL) theory [45,46]. The reduced temperature used in the analysis is [47]

$$\varepsilon = \left(T - T_c^{mf}\right) / \; T_c^{mf}. \quad (2)$$

Hence it is evident that the correct determination of T_c^{mf} is decisive in FLC and PG calculations. Importantly, the maximum of $d\rho/dT$ vs T, which corresponds to the inflection point (T_{inf}) of the resistive transition and often used as T_c^{mf} [39,41], is just the middle of the critical fluctuation region [42]. That is why an inequality $T_c^{mf} > T_{inf}$ must always take place [37,42,43]. Within the LP model it was convincingly shown that FLC measured for all without exception HTS's always demonstrates a crossover from 2D ($\xi_c(T) < d$) into 3D ($\xi_c(T) > d$) state as T draws near T_c ([9,43,44] and references therein). Here $\xi_c(T)$ is a coherence length along the c-axis and d is a distance between conducting layers in HTS's [47]. The result is most likely a consequence of Gaussian fluctuations of the order parameter in 2D metals which were found to prevent any phase coherency organization in 2D compounds [1,14]. As a result the critical temperature of an ideal 2D metal is found to be zero (Mermin–Wagner–Hoenberg theorem), and a finite value is obtained only when three-dimensional effects are taken into account [1,14,48–50]. That is why the FLC near T_c is always extrapolated by the standard equation of the Aslamasov–Larkin (AL) theory [51] with the critical exponent $\lambda = -1/2$ (Fig. 4, line 1) which determines the FLC in any 3D system

$$\sigma'_{AL3D} = C_{3D} \frac{e^2}{32\,\hbar \xi_c(0)} \varepsilon^{-1/\,2}, \quad (3)$$

where C_{3D} is a numerical factor used to fit the data by the theory [37,38]. This means that the conventional 3D FLC is realized in HTS's as $T \to T_c$ [37,44]. From Eq. (3), one can easy obtain $\sigma'^{-2} \sim \left(T - T_c^{mf}\right) / \; T_c^{mf}$. Evidently, $\sigma'^{-2} = 0$ when $T = T_c^{mf}$. This way of T_c^{mf} determination was proposed by Beasley [43] and justified in different FLC experiments [9,37,38]. Moreover, when T_c^{mf} is properly chosen the data in the 3D fluctuation region near T_c are always fitted by Eq. (3).

Fig. 3b displays the σ'^{-2} vs T plot for our sample H23 (dots). The interception of the extrapolated linear σ'^{-2} with T-axis determines $T_c^{mf} = 65.9$ K. Above the crossover temperature $T_0 = 68.5$ K the data deviates right from the line suggesting the 2D Maki–Thompson (MT) [52,53] fluctuation contribution into FLC [37]. Evidently, at the crossover temperature $\varepsilon_0 \sim T_0$ the coherence length $\xi_c(T) = \xi_c(0)\varepsilon^{-1/2}$ is expected to amount to d [9,37] which yields

$$\xi_c(0) = d\sqrt{\varepsilon_0}, \quad (4)$$

and allows the possibility of $\xi_c(0)$ determination. $\xi_c(0)$ is one of the important parameters of the PG analysis. Fig. 3 a demonstrates the same results (dots) for the sample H21 ($P = 0$).

Now, when T_c^{mf} is determined, the ln σ' vs ln ε can be plotted. The result is shown in Fig. 4b (circles) in comparison with the

Table 1
The parameters of the $HoB_2Cu_3O_{6.65}$ single crystal.

P (GPa)	ρ(100 K)(μΩ cm)	ρ(300 K)(μΩ cm)	T_c (K)	ΔT_c (K)	T_c^{mf} (K)	T^* (K)	T_0 (K)	$\xi_c(0)$ (Å)
0	186	838	61.3	2.3	61.9	269	64	2.13
0.48	159	715	63.2	4.0	65.9	265	68.5	2.33

Table 2
The parameters of the $HoB_2Cu_3O_{6.65}$ single crystal.

P (GPa)	T_{01} (K)	d_1 (Å)	C_{3D}	C_{2D}	T_G (K)	Gi	$\Delta^*(T_c)$ (K)	Δ^*_{max} (K)
0	99.5	2.74	1.9	2.18	62.3	0.006	154	272
0.48	114	2.71	1.5	1.9	67	0.017	157	258

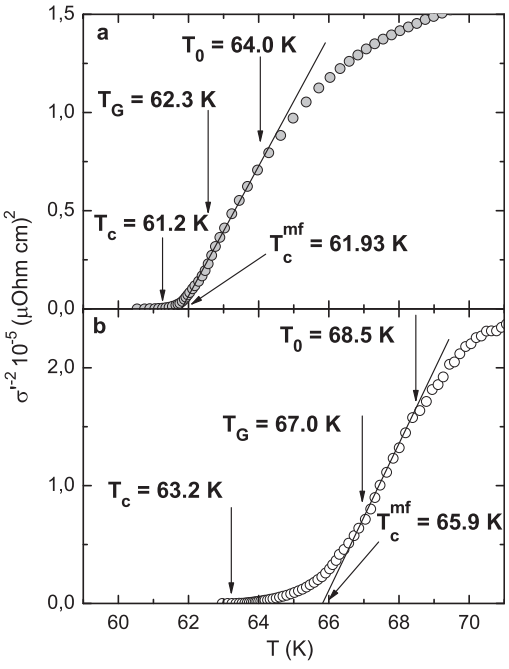

Fig. 3. σ'^{-2} as a function of T at $P = 0$ (a) and $P = 0.48$ GPa (b).

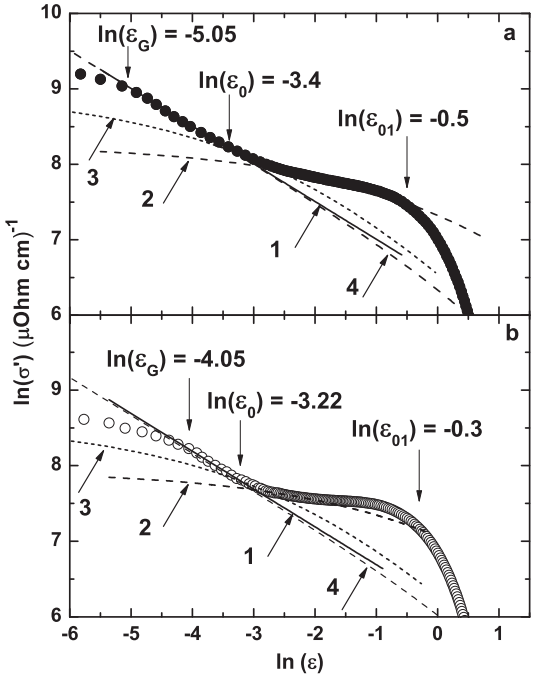

Fig. 4. ln σ' vs ln ε at $P = 0$ (dots, a) and $P = 0.48$ GPa (circles, b) compared with fluctuation theories: 1–3D AL; 2 – MT with $d = d_{01}$; 3 – MT with $d = 11.67$ Å; 4 – LD.

fluctuation theories. As expected above T_c^{mf} and up to $T_0 = 68.5$ K ($\ln\ \varepsilon_0 \approx -3.22$) σ' vs T is well extrapolated by the 3D fluctuation term (3) of the AL theory (Fig. 4b, solid line 1) with $\xi_c(0) = (2.33 \pm 0.01)$ Å determined by Eq. (4) and $C_{3D} = 1.5$ (see Table 2). Besides, by analogy with $YBa_2Cu_3O_{7-\delta}$ [37,40], we make use of $d = 11.67$ Å $= c$ which is the c-axis lattice parameter. Accordingly, above T_0 and up to $T_{01} \approx 114.7$ K ($\ln\ \varepsilon_{01} \approx -0.3$) σ' can be satisfactorily described by the MT fluctuation contribution (5) (Fig. 4b, dashed curve 2) of the Hikami–Larkin (HL) theory [47]

$$\sigma'_{MT} = \frac{e^2}{8d\,\hbar}\,\frac{1}{1-\alpha/\delta}\,\ln\left((\delta/\alpha)\,\frac{1+\alpha+\sqrt{1+2\alpha}}{1+\delta+\sqrt{1+2\delta}}\right)\,\varepsilon^{-1}, \tag{5}$$

which dominates well above T_c in the 2D fluctuation region [37,44,47]. In Eq. (5)

$$\alpha = 2\left[\frac{\xi_c(0)}{d}\right]^2\,\varepsilon^{-1}, \tag{6}$$

is a coupling parameter,

$$\delta = \beta\,\frac{16}{\pi\,\hbar}\left[\frac{\xi_c(0)}{d}\right]^2\,k_B T\tau_\phi, \tag{7}$$

is the pair-breaking parameter, and τ_ϕ that is defined by equation

$$\tau_\phi \beta\, T = \pi\hbar/8k_B\varepsilon = A/\varepsilon, \tag{8}$$

is the phase relaxation time, and $A = 2.998 \times 10^{-12}$ s K. The factor $\beta = 1.203(l/\ \xi_{ab})$, where l is the mean-free path and ξ_{ab} is the coherence length in the ab plane considering the clean limit approach ($l > \xi$) [9,37].

Unfortunately, neither l nor $\xi_{ab}(T)$ are measured in our experiments. To proceed with the analysis we will use the experimental fact that $\delta \approx 2$ when all other parameters are properly chosen [37]. Thus, to calculate the MT fluctuation contribution using Eq. (5) only the coupling parameter α (6) remains to be defined. To determine α we have to make use of another experimental fact that $\xi_c(0) = d\varepsilon_0^{1/2} = d_1\varepsilon_{01}^{1/2} = (2.33 \pm 0.01)$ Å [20,24]. Here d_1 corresponds to T_{01} and is a distance between conducting CuO_2 planes. Set $d = 11.67$ Å one can easy obtain $d_1 = d\sqrt{\varepsilon_0/\varepsilon_{01}} = 2.71$ Å which is actually the interplanar distance in $HoB_2Cu_3O_{6.65}$ ($d_1 \approx 3.0$ Å at optimal doping and $P = 0$ [54]). The finding suggests a conclusion that ε_{01} is properly chosen. Both ln ε_{01} and ln ε_0 are marked by the arrows in Fig. 4. Within this approach it is believed that below ε_{01} the $\xi_c(T) > d_1$ and couples the CuO_2 planes by Josephson interaction resulting in the appearance of the 2D FLC of MT type [9,44]. Thus, it turns out that just ε_{01} has to govern Eq. (7) and its proper choice is decisive for the FLC analysis. That is why we have to put

ε_{01} instead of ε_0 into Eq. (8) to find τ_ϕ (100 K) $\beta = (0.405 \pm 0.002) \times 10^{-13}$ s. If we use d = 11.67 Å and set $\varepsilon = \varepsilon_0$ in Eq. (8) it results in τ_ϕ (100 K) $\beta = (6.118 \pm 0.002) \times 10^{-13}$ s, and we will get curve 3 (Fig. 4b) which evidently does not meet the case. The result has to support the above considerations.

However, we have to emphasize that the latest approach with $d \approx 11.7$ Å and $\varepsilon = \varepsilon_0$ is widely used to analyze FLC in $YBa_2Cu_3O_{7-\delta}$ compounds [37,38,40] where no magnetism is expected. But, as can be seen from Fig. 4 (curves 3), if we use this approach in the case of $HoBa_2Cu_3O_{7-\delta}$ the theory is situated well below the data suggesting the enhanced MT fluctuation contribution into FLC compare with $YBa_2Cu_3O_{7-\delta}$. For the first time this enhanced MT fluctuation contribution resulting in necessity to use $d_1 \approx 3$ Å as a distance between conducting layers in HTS's instead of $d \approx 11.7$ Å was observed in the FLC analysis for FeAs-based magnetic superconductor $SmFeAsO_{0.85}$ [9,24]. Compare results we may conclude that the appreciable increase of the MT fluctuation contribution can be considered as a specific feature of the FLC behavior caused by the influence of $HoBa_2Cu_3O_{7-\delta}$ magnetic subsystem. As will be shown later the influence of magnetic subsystem is also seen in the pseudogap behavior of our $HoBa_2Cu_3O_{7-\delta}$ single crystals.

Lawrence and Doniach (LD) [55] have extended the initial AL calculations to a superconductor that consists of a stack of two-dimensional superconducting layers, linked by Josephson coupling between adjacent layers

$$\sigma'_{LD} = C_{LD} \frac{e^2}{16\,\hbar\, d} (1 + 2\alpha)^{-1/\,2} \varepsilon^{-1}, \tag{9}$$

This consideration resembles closely the situation in most HTS's, and the LD model is also used to describe FLC in HTS's ([38–40,42], and references therein). Obviously, near T_c, where $\xi_c(0) \gg d$ and $\alpha \gg 1$ (see Eq. (6)), the LD formula (9) reduces to the 3DAL Eq. (3). Accordingly at higher T, where $\xi_c(0) \ll d$ and $\alpha \ll 1$, Eq. (9) reduces to the classical 2DAL expression [37]. Thus the LD model demonstrates extended smooth 2D–3D transition as T approaches T_c [38]. This kind of FLC behavior was found to be typical for the HTS's systems with distorted sample structure [56], and we did not expect this behavior in our case. As expected above T_0 the LD curve (Fig. 4b, curve 4) deviates down from the 3DAL line (Fig. 4b, solid line) and drops far below the experimental data. It is in contrast with observed MT fluctuation contribution (Fig. 4b, curve 2) suggesting expected good quality of our sample crystal structure.

The similar ln σ' vs ln ε obtained within the same analysis for P = 0 is plotted in Fig. 4a (dots). As can be seen the LD model (Fig. 4a, curve 4) also does not meet the experimental case. On the contrary the data demonstrate very good fit with both 3DAL (Fig. 4a, straight line 1) and 2D enhanced MT (Fig. 4a, curve 2) theories in the whole temperature region of interest in a perfect agreement with above considerations. The finding is to justify proposed choice of ε_{01} within our approach. On the other hand, when pressure is applied only small part of the data between ln ε_0 and ln $\varepsilon \approx -1.96$ can be fitted by the MT theory in the proper way (Fig. 4b, curve 2). Above ln $\varepsilon \approx -1.96$ the data noticeably deviates upwards from the theory. Nevertheless, we still determine $\varepsilon_{01} = -0.3$ (Fig. 4b) as an intersection point between the theory and the data. Only this choice of ε_{01} allows us to get the self-consistent picture in calculating d_1 and $\xi_c(0)$, as mentioned above. Observed deviation is likely due to additional decrease of $\rho(T)$ under enhanced pressure (see Eq. (1)) and can be considered as a specific feature of the FLC behavior when current flows under an angle 45° to the **TB**. No such deviation of ln σ'(ln ε) from the enhanced MT contribution was observed under pressure for **I**||**TB** (sample S1) [20]. Moreover, in this case the best fit without any deviation of the data from MT theory was found just for P = 0.48 GPa [20] suggesting the opposite tendency of the FLC behavior when different geometry of measuring current direction is used.

Apart from evident decrease of resistivity and increase of T_c, T_c^{mf}, T_0 and T_{01} pressure leads to decrease of τ_ϕ (100 K)β, which is $(0.494 \pm 0.002) \times 10^{-13}$ s at P = 0, as well as of both C-factors (see the Tables). The closer C_{3D} to 1.0 the more homogeneous is the sample structure (see [9] and references therein). Thus, the reduction of the C-factors points out at the improvement of the sample structure under pressure. The conclusion is corroborated by the experimental fact that the temperature interval of the "Anderson"-type metal-to-dielectric (MD) transition, most likely caused by disorder in such systems [57], gradually decreases under pressure [33]. At the same time the absolute values of C_{3D} and C_{2D} are noticeably higher than those found in our previous experiment with **I**||**TB** [20]. At the latter case $C_{3D} = 0.53 - 1.1$ and $C_{2D} = 1.02 - 1.8$ were found at P = 0 and P = 0.48 GPa, respectively. Thus, observed increase of the C-factors supports the above idea of charge carrier scattering enhancement when current flows under an angle 45° to the **TB**. Besides an opposite tendency is observed in this case, namely both C-factors decrease with pressure.

As can be seen from the Tables, d_1 is only slightly reduces with pressure, whereas $\xi_c(0)$ is found to increase in good agreement with results obtained for different HTS's [30–32]. The increase is about 9.4% which is 2.5 times larger than 3.7% found for Hg-2223 [32] but 1.77 times less than that measured for $YBa_2Cu_3O_{7-\delta}$ [31] under the same pressure. This in turn will lead to an increase in the coupling constant α (6) or in the coupling strength $J = [\xi_c(0)/d]^2$ [31,32] for the neighboring CuO_2 planes. Simultaneously the range of critical fluctuation, $\Delta T_{cr} = T_G - T_c$, noticeably increases from 1.1 K at P = 0 up to 3.8 K at P = 0.48 GPa resulting in corresponding but modest decrease of the 3D AL fluctuation region, $T_0 - T_G$, from 1,7 K down to 1,5 K (Figs. 3, 4). Importantly, under pressure the width of the resistive transition, $\Delta T_c = T_c(0.9\rho'_N) - T_c(0.1\rho'_N)$ (Fig. 2), also increases in about 1.7 times (Table 1). Here $T_c(0.9\rho'_N)$ and $T_c(0.1\rho'_N)$ correspond to the temperatures at which resistivity decreases 10% and 90%, respectively, compare with its value ρ'_N just above the resistive transition designated by the upper straight line (Fig. 2).

The results allows us to consider the pressure effects on the extent of the critical fluctuation regime. Here T_G is a temperature generally accounted for by the Ginzburg criterium which is related to the breakdown of the mean-field GL theory to describe the superconducting transition as mentioned above [45,46,58]. Above T_c this criterium is identified to the lowest temperature limit for the validity of the Gaussian fluctuation region. In Figs. 3 and 4 we denote as T_G the crossover temperature delimiting the 3D Al fluctuation and critical intervals, and assign this temperature to the point where data deviate from the straight line. Having determined both T_G and T_c^{mf} for each applied pressure we may calculate the Ginzburg number, given as $Gi = (T_G - T_c^{mf})/T_c^{mf}$. Fig. 3a and b show that Gi noticeably increases with P (see also Table 2). Together with increase of ΔT_c and $\Delta\, T_{cr}$ it implies that the genuine critical fluctuations are enhanced when the pressure is applied. It appears to be somewhat surprising seeing the pressure is expected to improve the sample structure as discussed above, but the similar results have been obtained for OD $YBa_2Cu_3O_{7-\delta}$ single crystals [31] as well as for the sample S1 [20]. According to the anisotropic GL theory, the Ginzburg number is given as [58,59]

$$Gi = \alpha \left(\frac{k_B}{\Delta c \xi_c(0)\ \xi_{ab}(0)^2} \right)^2, \tag{10}$$

where α is a constant of the order 10^{-3} and Δc is the jump of the specific heat at T_c. According to the microscopic theory [59], $\Delta c \sim T_c N(0)$, where $N(0)$ is the single-particle density of states at

the Fermi level. Δc is expected to be weakly P dependent in this range since $N(0)$, as deduced from the Pauli susceptibility above T_c, is rather insensible to pressure in the HTS's [60]. The analysis of the FLC amplitude indicates the 9.4% increase of $\xi_c(0)$ under pressure. All findings suggest that the appreciable increase of Gi with pressure is likely due to a reduction in $\xi_{ab}(0)$. This is in accordance with prior findings [31,59] showing that independently of the sample composition and oxygen concentration the superconducting properties in HTS's depend much more on the variation of the atomic distances within the atomic layers than along the c-axis.

This seems to be reasonable since in the critical region $\Delta(T) < k_BT$ is assumed [1,45,46,58]. Apparently, the smaller $\xi_{ab}(T) = \xi_{ab}(0)(1 - T/T_c)^{-1/2}$ the less is $\Delta(T)$ [61] and the larger has to be the critical region. Nevertheless, the increase of both the Ginzburg number $Gi^* = Gi(P)/Gi(0) \approx 2,8$ and $\Delta T_{cr} \approx 3.8$ K is determined to be much larger than the corresponding parameters obtained for OD $YBa_2Cu_3O_{7-\delta}$ single crystals under the same pressure ($Gi^* \approx 1.25$ and $\Delta T_{cr} \approx 0.4$ K) [31]. Taking found increase of $\xi_c(0)$ into account from Eq. (9) we estimate that $\xi_{ab}(0)$ has to decrease by about 25% to produce the observed enhancement of Gi at $P = 0.48$ GPa. This is suspiciously large compare with 14% $\xi_{ab}(0)$ decrease determined for $YBa_2Cu_3O_{7-\delta}$ [31] and 7% $\xi_{ab}(0)$ decrease ensured from our analysis for $HoBa_2Cu_3O_{7-\delta}$ single crystals in the case of **I**||**TB** (sample S1) [20]. Additionally, in the last case the corresponding ΔT_c is about 3 times less and amounts only to $\Delta T_c = 0.7$ K and = 1.4 K at $P = 0$ and $P = 0.48$ GPa, respectively [20,33]. Moreover, in the case of **I**||**TB** $\Delta T_{cr} \approx 1$ K ($P = 0$) and ≈ 1.8 K ($P = 0.48$ GPa) it is more than twice smaller compared with the experiment geometry with the current passing under an angle 45° to the **TB**. We are thus led to conclude that both ΔT_{cr} and Gi increase not only as a consequence of the $\xi_{ab}(0)$ diminution under high pressure but also due to the n_f rearrangement caused by the change of the current flow direction comparatively to the **TB**. The results illustrate the significant role of the current flow direction in the processes of charge carriers scattering and possibly of the single crystal phase stratification especially in the slightly doped cuprates. We expected to find the similar specific features of this behavior analyzing the PG in our $HoBa_2Cu_3O_{7-\delta}$ single crystals.

3.2. Pseudogap analysis

A pseudogap in HTS's is manifested in resistivity measurements as a downturn of the longitudinal resistivity $\rho(T)$ at $T \leqslant T^*$ from its linear behavior above T^* [1–5,9]. This results in appearance of the excess conductivity $\sigma'(T) = \sigma(T) - \sigma_N(T)$ (see Eq. (1)). It is established [5,9,37] that the conventional fluctuation theories, modified for the HTS's by Hikami and Larkin (HL) [47], fit perfectly the experimental $\sigma'(T)$ but only up to approximately 110 K. Clearly, to attain information about the pseudogap we need an equation which specifies a whole experimental curve, from T_c up to T^*, and contains the PG in the explicit form. Besides, the dynamics of pair-creation $(1 - T/T^*)$ and pair-breaking $(\exp(-\Delta^*/T))$ (see Eq. (11)) above T_c must be taken into account in order to correctly describe the experiment [9,62]. Due to the absence of a complete fundamental theory the equation for $\sigma'(\varepsilon)$ has been proposed in Ref. [62] with respect to the local pairs:

$$\sigma'(\varepsilon) = \frac{e^2 A_4 \ (1 - \frac{T}{T^*})(exp(-\frac{\Delta^*}{T}))}{(16\ \hbar\xi_c(0)\sqrt{2\varepsilon^*_{c0}\ \sinh(2\varepsilon/\ \varepsilon^*_{c0})}}. \tag{11}$$

Here A_4 is a numerical factor which has the meaning of the C-factor in the fluctuation conductivity theory [9,37,38]. All other parameters, including the coherence length along the c-axis, $\xi_c(0)$, (Eq. (4)) and the theoretical parameter ε^*_{c0}, directly come from the experiment [9,62]. In the range $\ln \varepsilon_{01} < \ln \varepsilon < \ln \varepsilon_{02}$ (Fig. 5) or accordingly $\varepsilon_{01} < \varepsilon < \varepsilon_{02}$ (114 K < T < 135 K) (insert in Fig. 5),

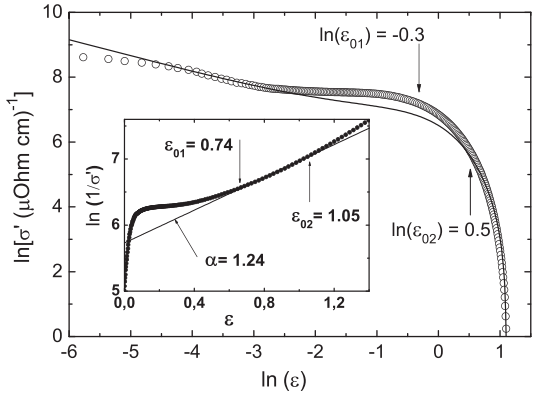

Fig. 5. ln σ'(ln ε) (circles) compared with Eq. (11) (solid line). Insert: ln σ'^{-1} as a function of ε. $P = 0.48$ GPa.

$\sigma'^{-1} \sim \exp(\varepsilon)$ [9,62]. As a result ln (σ'^{-1}) is a linear function of ε with a slope $\alpha^* = 1.24$ which determines parameter $\varepsilon^*_{c0} = 1/\alpha^*$ (insert in Fig. 5). To find A_4, we calculate $\sigma'(\varepsilon)$ using Eq. (11) and fit experiment in the range of 3D AL fluctuations near T_c (Fig. 5) where ln σ'(ln ε) is a linear function of the reduced temperature ε with a slope $\lambda = -1/2$. Besides, $\Delta^*(T_c) = \Delta(0)$ is assumed [62,63]. To estimate $\Delta^*(T_c)$, which we use in Eq. (11), we plot σ' as a function of $1/T$ [62,64] (Fig. 6). In this case the slope of the theoretical curve (Eq. (11)) turns out to be very sensitive to the value of $\Delta^*(T_c)$ [9,62]. The best fit is obtained when $2\Delta^*(T_c)/k_BT_c \approx 5.0$.

Solving Eq. (11) for the pseudogap $\Delta^*(T)$ one can readily obtain

$$\Delta^*(T) = T\ \ln\frac{e^2 A_4\ (1 - \frac{T}{T^*})}{\sigma'(T)16\ \hbar\xi_c(0)\sqrt{2\varepsilon^*_{c0}\ \sinh\left(2\varepsilon/\ \varepsilon^*_{c0}\right)}}. \tag{12}$$

Here $\sigma'(T)$ is the experimentally measured excess conductivity over the whole temperature interval from T^* down to T_c^{mf}. In Fig. 7 curve 1 is plotted for $P = 0$ using Eq. (12) with the following parameters derived from experiment: $\varepsilon^*_{c0} = 0.76, \xi_{c(0)} = 2.13$ Å, $T_c^{mf} = 61.9$ K, $T^* = 269$ K, $A_4 = 27.5$ and $\Delta^*(T_c)/k_B = 154$ K. Accordingly, curve 2 is plotted for $P = 0.48$ GPa with $\varepsilon^*_{c0} = 0.806$, $\xi_c(0) = 2.33$ Å, $T_c^{mf} = 65.9$ K, $T^* = 265$ K, $A_4 = 21$, $\Delta^*(T_c)/k_B = 157$ K (Table 1, 2). Importantly, if we substitute found $\Delta^*(T)$ into Eq. (11), independently on $P = 0$ or $P = 0.48$ GPa, the resulting curve will exactly describe the $\sigma'(T)$ data.

As can be observed from the figure, at $P = 0$ function $\Delta^*(T)$ exhibits two unexpected maxima at $T_{m1} \approx 219\ K$ and at $T_{m2} \approx 241\ K$ (Fig. 7, curve 1). The maximum at the higher T is sufficiently pronounced. The maxima appear most likely because of

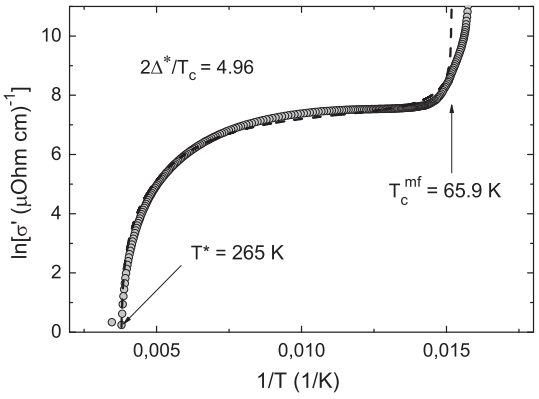

Fig. 6. ln σ' vs $1/T$ (circles) compared with Eq. (11) (dashed line) plotted with $\Delta^*(T_c) = 156.7$ K. $P = 0.48$ GPa.

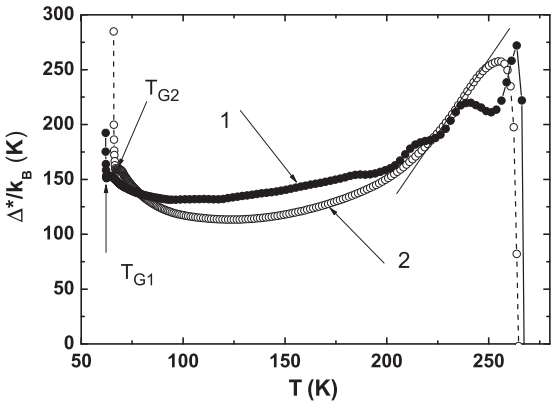

Fig. 7. Δ^*/k_B as a function of T. Dots (1) – $P = 0$; circles (2) – $P = 0.48$ GPa.

two-phase stratification of the single crystal [26,27,33]. Induced by the pressure, an increase in the amplification process of ascending diffusion in the sample, which leads to redistribution of labile oxygen from the charge depleted low temperature phase to the high temperature one [33,35], results in disappearance of these maxima and emergence of a linear dependence $\Delta^*(T)$ with a positive slope near high temperatures (curve 2). One of the possible reason of the phase separation could be the origin of the low T_c in the **TB** boundaries. Experiments on the vortex structure [65,66] have shown that the density of vortices in the **TB** increases in comparison to their density in the volume of the superconductor, indicating the suppression of T_c in the **TB**. This may be due to the low oxygen concentration in the **TB** plane, which effectively implies a high concentration of oxygen vacancies [67] as a consequence of mechanical tensions. Notably, below T_G the sample transforms into the critical fluctuation region, and data sharply deviate upwards from the LP model description. The LP model approach is very sensitive. Really, no corresponding peculiarities are seen neither on $\rho(T)$ nor on $\ln\ \sigma'(\ln\ \varepsilon)$ in the temperature range where the maxima on $\Delta^*(T)$ are observed.

Nevertheless, in contrast with **I**||**TB**, the maxima only slightly suppressed when pressure is firstly applied. To get the complete maxima suppression, as shown by curve 2 in Fig. 7, we have to wait several days. It means that the specific current carrier distribution realized in this case [33,35] somehow prevents to the process of ascending diffusion in the sample. In the case of **I**||**TB** the maxima have been suppressed immediately after the pressure has been applied [20]. Moreover, the maxima are determined to move apart toward high temperatures compare with **I**||**TB**. The shift is ≈ 24 K for the lower maximum and about 31 K for the upper one which is comparable with the shift of $T^* \approx 27$ K. Besides, the distance between the maxima $\Delta T_m \approx 21$ K is about 6 K larger now. Note that the maxima of $\Delta^*(T)$ and initial values of ρ, T_c and $\xi_c(0)$ are restored when the pressure is removed thus confirming the assumption as for ascending diffusion [33–35]. Again the final restoration is achieved only after several days without pressure. The findings emphasize the difference in the sample behavior when the current flow direction is changed.

Summarizing results we may conclude that both $\sigma'(T)$ and $\Delta^*(T)$ are markedly different from those obtained for the $YBa_2Cu_3O_{7-\delta}$ films with different oxygen content [9,62] where no magnetism is expected. At the same time they resemble similar $\sigma'(T)$ and $\Delta^*(T)$ found for FeAs-based superconductor $SmFeAsO_{0.85}$ [9,24] where the magnetic fluctuations are believed to play a significant role (see Ref. [9] and references therein). Thus, found peculiarities of the FLC and PG behavior are believed to be explained by the influence of paramagnetism in $HoBa_2Cu_3O_{7-\delta}$ [68] as well as by the possibility of strengthening some specific mechanisms of the quasiparticle interaction in these compounds [69–71]. At any rate the issue requires futher investigation.

4. Conclusion

We present a detailed consideration of the influence of the high pressure on the different properties of the slightly oxygen deficient $HoBa_2Cu_3O_{7-\delta}$ single crystals including the fluctuation conductivity and pseudogap. The change of the samples parameters under pressure are determined to be more pronounced as compared with $YBa_2Cu_3O_{7-\delta}$ [31,34]. This is because the substitution of yttrium with holmium (which has a larger ionic radius than Y and besides is believed to possess magnetic properties) significantly affects the charge distribution and effective interaction in the CuO_2 planes, thereby stimulating the disordering in the oxygen subsystem which is affected by pressure. Twin boundaries, being typical for the slightly doped single crystals, are also shown to be the effective scattering centers of normal carriers in $HoBa_2Cu_3O_{7-\delta}$ compounds. Their influence on the charge distribution is reasonably pronounced and play any significant role only in the case of measuring current flow under an angle 45° to the **TB**. On the other hand, the **TB**, being the regions with lowered T_c most likely because of the lowered oxygen concentration in the TB planes, actively participate in the process of single crystal phase stratification [33–35].

As a result noticeably enhanced MT fluctuation contribution into FLC, which becomes more pronounced under pressure, is observer in the 2D fluctuation region near T_c. Simultaneously $\Delta^*(T)$ exhibits two maxima at $T_{m1} \approx 219$ K and at $T_{m2} \approx 241$ K at $P = 0$ most likely just because of this two-phase stratification of the sample [26,27,33]. Induced by the pressure, the redistribution of labile oxygen enhances phase separation in the single crystal and thereby stimulates ascending diffusion processes between the superconducting phases with different oxygen stoichiometry. This leads to the disappearance of the maxima (but after five days under pressure) and the emergence of a linear dependence $\Delta^*(T)$ with a positive slope near high temperatures. Simultaneously the main part of sample parameters, especially $\Delta T_c, \Delta T_{cr}, T_G$ and Ginzburg number Gi, increases significantly. Importantly, the maxima on $\Delta^*(T)$ and initial values of all other parameters are restored when the pressure is removed thus confirming the assumption as for ascending diffusion.

Eventually we may conclude that both $\sigma'(T)$ and $\Delta^*(T)$ are markedly different from those obtained for the $YBa_2Cu_3O_{7-\delta}$ films with different oxygen content [9,62] where no magnetism is expected. At the same time they resemble analogous $\sigma'(T)$ and $\Delta^*(T)$ dependencies found for FeAs-based superconductor $SmFeAsO_{0.85}$ where the magnetic fluctuations are believed to play a significant role. It seems to be very tempting to account for the found peculiarities of the FLC and PG behavior by the influence of paramagnetism in $HoBa_2Cu_3O_{7-\delta}$.

Acknowledgement

This work was supported in part by European Commission CORDIS Seven Framework Program, Project No. 247556.

References

[1] V.M. Loktev, Low Temp. Phys. 22 (1996) 488.
[2] A.A. Pashitskii, Low Temp. Phys. 21 (1995) 763;
A.A. Pashitskii, Low Temp. Phys. 21 (1995) 837.
[3] B.P. Stojkovic, D. Pines, Phys. Rev. B 55 (1997) 8576.
[4] E.G. Maksimov, Physics-Uspekhi 43 (2000) 965.
[5] T. Timusk, B. Statt, Rep. Prog. Phys. 62 (1999) 161.
[6] K. Nakayama, T. Sato, Y. Sekiba, K. Terashima, P. Richard, T. Takahashi, K. Kudo, N. Okumura, T. Sasaki, N. Kobayashi, Phys. Rev. Lett. 102 (2009) 227006.
[7] K. Nakayama, T. Sato, Y.-M. Xu, Z.-H. Pan et al., arXiv:1105.5865v [cond-mat, supr-con].

[8] Rui-Hua He, M. Hashimoto, H. Karapetyan, J.D. Koralek, et al., Science 331 (2011) 1579.
[9] A.L. Solovjov, Superconductors – Materials, Properties and Applications. Chapter 7: Pseudogap and local pairs in high-Tc superconductors, InTech, Rijeka, pp. 137, 2012.
[10] M.A. Obolenskii, R.V. Vovk, A.V. Bondarenko, N.N. Chebotaev, Low Temp. Phys. 32 (2006) 571.
[11] R. Combescot, X. Leyronas, M. Yu Kagan, Phys. Rev. A 73 (2006) 023618.
[12] V.J. Emery, S.A. Kivelson, Nature (London) 374 (1995) 434.
[13] Q. Chen, I. Kosztin, B. Janko, K. Levin, Phys. Rev. Lett. 81 (1998) 4708.
[14] J.R. Engelbrecht, A. Nazarenko, M. Randeria, E. Dagotto, Phys. Rev. B 57 (1998) 13406.
[15] A.V. Chubukov, J. Schmalian, Phys. Rev. B 57 R11 (1998) 085.
[16] P.W. Anderson, J. Phys.: Condens. Matter. 8 (10) (1996) 083.
[17] P.A. Lee, Physica C 317–318 (1999) 194.
[18] Y. Ando, S. Komiya, K. Segawa, S. Ono, Y. Kurita, Phys. Rev. Lett. 93 (2004) 267001.
[19] T. Ito, K. Takenaka, S. Uchida, Phys. Rev. Lett. 70 (1993) 3995.
[20] A.L. Solovjov, M.A. Tkachenko, R.V. Vovk, M.A. Obolenskii, Low Temp. Phys. 37 (2011) 840.
[21] A.L. Solovjov, M.A. Tkachenko, 1112.3812v1 [cond-mat,supr-con].
[22] K. Machida, K. Nokura, T. Matsubara, Phys. Rev. B 22 (1980) 2307.
[23] H. Chi, A.D.S. Nagi, J. Low Temp. Phys. 86 (1992) 139.
[24] A.L. Solovjov, V.N. Svetlov, V.B. Stepanov, S.L. Sidorov, V. Yu. Tarenkov, A.I. D'yachenko, A.B. Agafonov, arXiv:1012.1252v [cond-mat,supr-con].
[25] B.N. Goshchitskii, V.L. Kozhevnikov, M.V. Sadovskii, Int. J. Mod. Phys. B2 (1988) 1331.
[26] R.V. Vovk, M.A. Obolenskii, A.A. Zavgorodniy, I.L. Goulatis, V.I. Beletskii, A. Chroneos, Physica C 469 (2009) 203.
[27] R.V. Vovk, M.A. Obolenskii, A.A. Zavgorodniy, A.V. Bondarenko, I.L. Goulatis, A.V. Samoilov, A.I. Chroneos, J. Alloys Comp. 453 (2008) 69.
[28] C.W. Chu, P.H. Hor, R.L. Meng, L. Gao, A.J. Huang, Y.Q. Wang, Phys. Rev. Lett. 58 (1988) 405.
[29] H.J. Liu, Q. Wang, G.A. Saunders, D.P. Almond, B. Chapman, K. Kitahama, Phys. Rev. B 51 (1995) 9167.
[30] Q. Wang, G.A. Saunders, H.J. Liu, M.S. Acres, D.P. Almond, Phys. Rev. B 55 (1997) 8529.
[31] L.M. Ferreira, P. Pureur, H.A. Borges, P. Lejay, Phys. Rev. B 69 (2004) 212505.
[32] L.J. Shen, C.C. Lam, J.Q. Li, J. Feng, Y.S. Chen, H.M. Shao, Supercond. Sci. Technol. 11 (1998) 1277.
[33] R.V. Vovk, Z.F. Nazyrov, M.A. Obolenskii, I.L. Goulatis, A. Chroneos, V.M. Pinto Simoes, Philos. Mag. 91 (2011) 2291.
[34] R.V. Vovk, M.A. Obolenskii, Z.F. Nazyrov, I.L. Goulatis, A. Chroneos, V.M. Pinto Simoes, J. Mater Sci.: Mater. Electron. 23 (2012) 1255.
[35] R.V. Vovk, A.A. Zavgorodniy, M.A. Obolenskii, I.L. Goulatis, A. Chroneos, V.P. Pinto Simoes, J. Mater. Sci. Mater. Electron. 22 (2011) 20.
[36] J.D. Thompson, Rev. Sci. Instrum. 55 (1984) 231.
[37] A.L. Solovjov, H.-U. Habermeier, T. Haage, Low Temp. Phys. 28 (2002) 22; A.L. Solovjov, H.-U. Habermeier, T. Haage, Low Temp. Phys. 28 (2002) 144.
[38] B. Oh, K. Char, A.D. Kent, M. Naito, M.R. Beasley, et al., Phys. Rev. B 37 (1988) 7861.
[39] R.K. Nkum, W.R. Datars, Phys. Rev. B 44 (1991) 12516.
[40] W. Lang, G. Heine, P. Schwab, X.Z. Wang, D. Bauerle, Phys. Rev. B 49 (1994) 4209.
[41] E.V.L. de Mello, M.T.D. Orlando, J.L. Gonzalez, E.S. Caixeiro, E. Baggio-Saitovich, Phys. Rev. B 66 (2002) 092504.
[42] J.A. Veira, Felix Vidal, Physica C 159 (1989) 468.
[43] M.R. Beasley, Physica B 148 (1987) 191.
[44] Y.B. Xie, Phys. Rev. B 46 (1992) 13997.
[45] V.L. Ginzburg, L.D. Landau, JETP 20 (1950) 1064.
[46] E.M. Lifshitz, L.P. Pitaevski, Statistical Physics, Vol. 2, Moscow: Nauka, 1978.
[47] S. Hikami, A.I. Larkin, Mod. Phys. Lett. B 2 (1988) 693.
[48] R. Haussmann, Phys. Rev. B 49 (1994) 12975.
[49] J.R. Engelbrecht, M. Randeria, C.A.R. Sa de Melo, Phys. Rev. B 55 (1997) 15153.
[50] O. Tchernyshyov, Phys. Rev. B 56 (1997) 3372.
[51] L.G. Aslamazov, A.L. Larkin, Phys. Lett. 26A (1968) 238.
[52] K. Maki, Prog. Theor. Phys. 39 (1968) 897.
[53] R.S. Thompson, Phys. Rev. B 1 (1970) 327.
[54] G.D. Chryssikos, E.I. Kamitsos, J.A. Kapoutsis, et al., Physica C 254 (1995) 44.
[55] W.E. Lawrence, S. Doniach, in: E. Kanda (Ed.) Proceedings of the Twelfth Int. Conf. on Low Temp. Phys., Kyoto, 1970 (Keigaku, Tokyo, 1971), pp. 361.
[56] A.L. Solovjov, Low Temp. Phys. 28 (2002) 812.
[57] N.F. Mott, Metal-Insulator Transition, World Scientific, London, 1974.
[58] A. Kapitulnik, M.R. Beasley, C. Castellani, C. Di Castro, Phys. Rev. B 37 (1988) 537.
[59] T. Schneider, J.M. Singer, Phase Transition Approach to High Temperature Superconductivity: Universal Properties of Cuprate Superconductors, Imperial College Press, London, 2000.
[60] J.S. Schilling, S. Klotz, Physical Properties of High Temperature Superconductors, in: D.M. Ginsberg (Ed.), 3, World Scientific, Singapore, 1992, p. 59.
[61] P.G. De Gennes, Superconductivity of Metals and Alloys, W.A. Benjamin, INC.,, New York – Amsterdam, 1966. pp. 280.
[62] A.L. Solovjov, V.M. Dmitriev, Low Temp. Phys. 32 (2006) 99.
[63] E. Stajic, A. Iyengar, K. Levin, B.R. Boyce, T.R. Lemberger, Phys. Rev. B 68 (2003) 024520.
[64] D.D. Prokofev, M.P. Volkov, Yu. A. Bojkov, Fiz. Tverd. Tela 45 (2003) 11.
[65] L. Ya Vinnikov, L.A. Gurevich, G.A. Yemelchenko, Yu A. Ossipyan, Solid State Commun. 67 (1988) 421.
[66] C. Duran, P.L. Gammel, R. Wolfe, Nature 357 (1992) 474.
[67] G. Blatter, M.V. Feigelman, V.B. Geshkenbein, A.I. Larkin, V.M. Vinokur, Rev. Mod. Phys. 66 (1994) 1125.
[68] A.J. Drew, Ch. Niedermayer, P.J. Baker, F.L. Pratt, et al., Nat. Mater. 8 (2009) 310.
[69] V.M. Apalkov, M.E. Portnoi, Phys. Rev. B (2002). 66121303 (R).
[70] R.V. Vovk, N.R. Vovk, O.V. Shekhovtsov, I.L. Goulatis, A. Chroneos, Supercond. Sci. Technol. 26 (2013) 085017.
[71] P.G. Curran, V.V. Khotkevych, S.J. Bending, A.S. Gibbs, S.L. Lee, A.P. Mackenzie, Phys. Rev. B 84 (2011) 104507.